Color Effect on the Face Recognition with Spatial Resolution Constraints

Jae Young Choi[1,2], Seungji Yang[1], Yong Man Ro[1,2], Konstantinos N. Plataniotis[2]
[1]*Image and Video System Laboratory, Information and Communication University,*
[2]*Department of Electrical and Computer Engineering, University of Toronto*
vanchoi@icu.ac.kr

Abstract

In the practical face recognition (FR) applications, low-resolution faces (20 x 20 pixels or less) are commonly encountered and negatively impact on reliable performance. To overcome low-resolution face problem, we show that face color can significantly improve the performance compared to intensity-based features. The contribution of this paper is twofold. First, a new metric called 'variation ratio gain' (VRG) is proposed to theoretically prove the significance of color effect on low-resolution faces. Second, we conduct extensive performance comparison studies. In particular, 3,192 color facial images corresponding to 341 subjects, collected from three standard CMU PIE, FERET, and XM2VTSDB face databases, were used to perform comparative studies of color effect on various face resolutions. Experimental results verified that face color feature improves the degraded recognition rate due to low-resolution faces by at least an order of magnitude over intensity-based features.

1. Introduction

Face recognition technologies are being revisited toward Multimedia Information Retrieval (MIR) [1]. With increasing demands of automatic annotation of faces for personal photos, snap-shot images and video clips offered via Web services, FR technologies have been central part for reliable annotation of faces on various multimedia contents. Despite recent growth, precise FR is still a tough task due to faces captured from various environments including illumination, pose, aging, and resolution variations. In particular, many current FR-based multimedia applications often suffer from small-sized faces (20×20 pixels or less) [2-4] from limited capturing conditions, e.g., faces captured from long distance cameras or camera-phones.

Some FR literatures dealt with face resolution problem [2-3], [5-7]. In [2], 15×15 pixels is considered to be as a minimum face resolution for reliable detection and recognition of faces. The CHIL project [5] reported that normal face resolution in video-based FR (e.g., video surveillance) is 10 to 20 pixels in the eye distance and face region is usually $1/16^{th}$ of commonly used TV recording resolution of 320×240 pixels. Further, FRVT 2000 [3] studied the effect of resolution on performance until eye distance is as low as 5×5 pixels. In addition, previous works examined how low-resolution gray-scale (or intensity) faces affect recognition performance. They revealed that much lower resolution faces significantly deteriorated the recognition performance comparing with high-resolution ones [3], [6-7].

Evidently, low-resolution faces impose a significant restriction on the conventional intensity-based FR systems to guarantee reliability and feasiability. Traditional resolution enhancement techniques such as 'super-resolution' could be used to handle low-resolution faces. One significant disadvantage, however, is that these techniques require multiple low-resolution facial images that belong to the same identity captured from the same scene. In practice, it is usually difficult to support such requirement (e.g., only a single face image of being the same person is usually available for annotation of faces on personal photos). To circumvent the problem due to low-resolution faces, selecting face features robust to changes in face resolution is critically important. In contrast to the intensity-driven features, color cue is known to be less susceptible to resolution changes [8]. In addition, the psychophysical result of the FR test in Human Visual System (HVS) showed that the contribution of color cue would be more evident when the shapes of face were degraded [9]. Usefulness of color in the computerized FR systems was demonstrated in many literatures [10-13]. They mainly focused on following issues: was color information helpful to improve the performance in comparison to gray-scale only [10-13]; how three spectral channels of color were utilized [10], [12]; which color space was the best [11-12]. However, color effect on face resolution has not yet been fully investigated in the current color-based FR works and

978-0-7695-3454-1/08 $25.00 © 2008 IEEE
DOI 10.1109/ISM.2008.22

no paper suggests the useful color FR framework robust against low-resolution faces.

In this paper, we investigate how the face color cue contributes to the performance as the face resolution is extremely changed in two de factor FR methods - Principal Component Analysis [14] (PCA or "eigenface") and Linear Discriminant Analysis [15] (LDA or "fisherface"). Especially, we show the significant impact of color on low-resolution faces by comparing the performance between color and gray-scale features. For theoretical analysis, color face representation model is built up in which face vector is defined as an augmented column vector by each spectral component of color face. Within this model, Variation Ratio Gain (VRG) is proposed to analyze the contribution of color to the performance with respect to face resolution changes. The effectiveness of color in FR scenario confronted with much lower resolution faces has been tested using three well-known standard data sets from CMU PIE [16], FERET [17], and XM2VTSDB [18]. According to experimental results, efficient use of color feature drastically reduces lower bound of face resolution to be reliably recognizable in the computer FR beyond what is possible with intensity-based features.

The rest of paper is organized as follows: the next section introduces the proposed color FR framework. In Section 3, we first introduce variation ratio and then make theoretical analysis to explain the effect of color on variation ratio. In Section 4, based on analysis made in Section 3, VRG is proposed to provide a theoretical insight on the relationship between color effects and face resolution. Section 5 presents the results of extensive experiments performed to demonstrate the effectiveness of color on low-resolution face. Conclusion is drawn in Section 6.

2. Color augmentation based subspace face recognition

In this section, we formulate a base-line color FR framework [12] to analyze color effect on face resolution. Given a color face image I, let s_m be a m^{th} spectral component vector of I (in form of column vector by lexicographic ordering of pixel elements of two-dimensional spectral images), where $\mathrm{s}_m \in \mathbf{R}^{N_m}$ and $\mathbf{R}^{N_m}$ denotes N_m-dimensional real space. Then, face vector is defined as an augmentation (or combination) of each spectral component s_m such that $\mathrm{x} = [\mathrm{s}_1^{\mathrm{T}} \ \mathrm{s}_2^{\mathrm{T}} \ \cdots \ \mathrm{s}_K^{\mathrm{T}}]^{\mathrm{T}}$, where $\mathrm{x} \in \mathbf{R}^N$, $N = \sum_{m=1}^{K} N_m$, and T denotes transpose operator. Face vector can be generalized in that, for $K = 1$, the face vector is defined by gray-scale only while, for $K = 3$, it is defined by spectral component configuration like $\mathrm{YC_bC_r}$ or $\mathrm{YQC_r}$ by column order.

The most of subspace FR methods is separately divided into training and testing stages. In the training stage, I is first rescaled into the prototype template size to be used for creation of face vector. With a formed training set, feature subspace is trained and constructed. Rational behind the feature subspace is to find a transformation φ by optimizing criteria, which produces a low-dimensional feature representation $\mathrm{f} = \varphi(\mathrm{x})$, where $\mathrm{f}_i \in \mathbf{R}^F$ and $F << N$. For testing unknown faces, let $\mathrm{G} = \{\mathrm{g}_i\}_{i=1}^{H}$ be a gallery set, which is a set of H prototype enrolled face vectors of known individuals, where $\mathrm{g}_i \in \mathbf{R}^N$. Let p be an unknown face vector to be identified, denoted as probe, where $\mathrm{p} \in \mathbf{R}^N$. In the testing stage, both g_i $(i = 1,\ldots,H)$ and p are projected onto the feature subspace to get the corresponding feature representations. A nearest neighbor classifier is then applied to determine the identity of p by comparing the distance between g_i and p in the feature subspace.

3. Analysis of color effect in subspace face recognition

Wang *et al.* [19] proposed face difference model that establishes unified framework of PCA and LDA. Based on this model, intra- and extra-personal variations are important factors to determine performance in PCA and LDA. These two factors can be measured by variation ratio [20]. Before analyzing color effect on face resolution, we begin by introducing variation ratio and exploit how color affects on variation ratio in PCA[1].

3.1. Variation ratio

Given a training set $\{\mathrm{x}_i\}_{i=1}^{M}$ of M face vector samples, covariance matrix C in PCA is computed from all the difference between any two face vectors [19] such that

[1] In this paper, theoretical analysis is given in only PCA framework. However, our analysis is easily applied to LDA due to the same intrinsic connection of intra- and extra-personal variations proposed in [19].

$$\mathrm{C} = \sum_{i=1}^{M}\sum_{j=1}^{M}(\mathrm{x}_i - \mathrm{x}_j)(\mathrm{x}_i - \mathrm{x}_j)^{\mathrm{T}}. \quad (1)$$

The C is decomposed into intra- (within-) and extra-personal (between-class) covariance matrices [19] denoted as IC and EC, respectively. Then, IC and EC are defined as

$$\begin{aligned}\mathrm{IC} &= \sum_{l(\mathrm{x}_i)=l(\mathrm{x}_j)}(\mathrm{x}_i - \mathrm{x}_j)(\mathrm{x}_i - \mathrm{x}_j)^{\mathrm{T}} \text{ and}\\ \mathrm{EC} &= \sum_{l(\mathrm{x}_i)\neq l(\mathrm{x}_j)}(\mathrm{x}_i - \mathrm{x}_j)(\mathrm{x}_i - \mathrm{x}_j)^{\mathrm{T}}.\end{aligned} \quad (2)$$

where $l(\cdot)$ returns a class label of x_i.

From a classification point of view, recognition performance can be enhanced as the extracted feature subspace learns and includes larger variation of EC than that of IC [19-20]. Obviously, the ratio of extra- to intra-personal variations can be adopted as an important parameter that reflects discriminative power of feature subspace in PCA. To define variation ratio, let Φ be an eigenvector matrix of C. Then, intra- and extra-personal variations of feature subspace spanned by Φ are computed as [20]

$$\begin{aligned}\mathrm{Var}_{\Phi}(\mathrm{IC}) &= \mathrm{tr}\,(\Phi^{\mathrm{T}}\,\mathrm{IC}\,\Phi\,) \text{ and}\\ \mathrm{Var}_{\Phi}(\mathrm{EC}) &= \mathrm{tr}\,(\Phi^{\mathrm{T}}\,\mathrm{EC}\,\Phi\,),\end{aligned} \quad (3)$$

where $\mathrm{Var}_{\Phi}(\mathrm{IC})$ and $\mathrm{Var}_{\Phi}(\mathrm{EC})$ denote intra- and extra-personal variations, respectively and $\mathrm{tr}(\cdot)$ is trace operator of matrix. Using Eq. (3), the variation ratio J is defined as

$$\mathrm{J} = \frac{\mathrm{Var}_{\Phi}(\mathrm{EC})}{\mathrm{Var}_{\Phi}(\mathrm{IC})}. \quad (4)$$

As J increases, the trained feature subspace relatively contains larger variation of EC compared to IC. Thus, it can represent well discriminative capability of feature subspace for classification task.

3.2. The color effect on variation ratio

In the color augmentation based subspace FR, x_i is usually composed of three different spectral components of I due to better performance than combination of two different spectral components reported in [11]. In the following, x_i is assumed to be the configuration of one luminance (s_{i1}) and two different chrominances (s_{i2} and s_{i3}) vectors such that $\mathrm{x}_i = [\mathrm{s}_{i1}^{\mathrm{T}}\ \mathrm{s}_{i2}^{\mathrm{T}}\ \mathrm{s}_{i3}^{\mathrm{T}}]^{\mathrm{T}}$. Using Eq. (1) and definition of x_i, C is written as

$$\mathrm{C} = \begin{bmatrix}\mathrm{C}_{11} & \mathrm{C}_{12} & \mathrm{C}_{13}\\ \mathrm{C}_{21} & \mathrm{C}_{22} & \mathrm{C}_{23}\\ \mathrm{C}_{31} & \mathrm{C}_{32} & \mathrm{C}_{33}\end{bmatrix}, \quad (5)$$

where $\mathrm{C}_{mn} = \sum_{i=1}^{M}\sum_{j=1}^{M}(\mathrm{s}_{im} - \mathrm{s}_{jm})(\mathrm{s}_{in} - \mathrm{s}_{jn})^{\mathrm{T}}$ and $(m, n = 1,2,3)$. In Eq. (5), C is a block covariance matrix whose entries are partitioned into covariance or cross-covariance sub-matrices C_{mn}. For $m = n$, C_{mn} is a covariance sub-matrix computed from a set $\{\mathrm{s}_{im}\}_{i=1}^{M}$, otherwise $m \neq n$, C_{mn} is a cross-covariance sub-matrix computed between $\{\mathrm{s}_{im}\}_{i=1}^{M}$ and $\{\mathrm{s}_{in}\}_{i=1}^{M}$, where $\mathrm{C}_{mn} = \mathrm{C}_{nm}^{\mathrm{T}}$. From Eq. (2), C in Eq. (5) is decomposed into IC and EC

$$\begin{aligned}\mathrm{IC} &= \begin{bmatrix}\mathrm{IC}_{11} & \mathrm{IC}_{12} & \mathrm{IC}_{13}\\ \mathrm{IC}_{21} & \mathrm{IC}_{22} & \mathrm{IC}_{23}\\ \mathrm{IC}_{31} & \mathrm{IC}_{32} & \mathrm{IC}_{33}\end{bmatrix} \text{ and}\\ \mathrm{EC} &= \begin{bmatrix}\mathrm{EC}_{11} & \mathrm{EC}_{12} & \mathrm{EC}_{13}\\ \mathrm{EC}_{21} & \mathrm{EC}_{22} & \mathrm{EC}_{23}\\ \mathrm{EC}_{31} & \mathrm{EC}_{32} & \mathrm{EC}_{33}\end{bmatrix},\end{aligned} \quad (6)$$

where IC_{mn} and EC_{mn} are

$$\begin{aligned}\mathrm{IC}_{mn} &= \sum_{l(\mathrm{x}_i)=l(\mathrm{x}_j)}(\mathrm{s}_{im} - \mathrm{s}_{jm})(\mathrm{s}_{in} - \mathrm{s}_{jn})^{\mathrm{T}} \text{ and}\\ \mathrm{EC}_{mn} &= \sum_{l(\mathrm{x}_i)\neq l(\mathrm{x}_j)}(\mathrm{s}_{im} - \mathrm{s}_{jm})(\mathrm{s}_{in} - \mathrm{s}_{jn})^{\mathrm{T}}.\end{aligned} \quad (7)$$

In Eq. (6), IC and EC are also block covariance matrices whose entries are partitioned into covariance or cross-covariance sub-matrices IC_{mn} and EC_{mn} $(m, n = 1,2,3)$, respectively.

Now we investigate color effect on variation ratio by calculating the variations of IC and EC in Eq. (6). By the proof given in Appendix section, traces of IC and EC are computed as

$$\begin{aligned}\mathrm{tr}(\mathrm{IC}) &= \sum_{m=1}^{3}\mathrm{tr}(\mathrm{I}\Lambda_{mm}) \text{ and}\\ \mathrm{tr}(\mathrm{EC}) &= \sum_{m=1}^{3}\mathrm{tr}(\mathrm{E}\Lambda_{mm}),\end{aligned} \quad (8)$$

where $I\Lambda_{mm}$ and $E\Lambda_{mm}$ are diagonal eigenvalue matrices of IC_{mm} and EC_{mm}, respectively. Using Eq. (3) and cyclic property of trace, variations of IC and EC are computed as

$$\begin{aligned} \mathrm{Var}_{\Phi}(\mathrm{IC}) &= \mathrm{tr}(\Phi\Phi^{\mathrm{T}}\mathrm{IC}) = \mathrm{tr}(\mathrm{IC}) \text{ and} \\ \mathrm{Var}_{\Phi}(\mathrm{EC}) &= \mathrm{tr}(\Phi\Phi^{\mathrm{T}}\mathrm{EC}) = \mathrm{tr}(\mathrm{EC}), \end{aligned} \tag{9}$$

where Φ is an eigenvector matrix of C shown in Eq. (5). Like Eq. (9), the variations of IC_{mm} and EC_{mm} are also computed as

$$\begin{aligned} \mathrm{Var}_{\Phi_{mm}}(\mathrm{IC}_{mm}) &= \mathrm{tr}(\mathrm{I}\Lambda_{mm}) \text{ and} \\ \mathrm{Var}_{\Phi_{mm}}(\mathrm{EC}_{mm}) &= \mathrm{tr}(\mathrm{E}\Lambda_{mm}), \end{aligned} \tag{10}$$

where Φ_{mm} is an eigenvector matrix of C_{mm} and $m = 1, 2, 3.$

Substituting Eq. (9) and (10) into Eq. (8), $\mathrm{Var}_{\Phi}(\mathrm{IC})$ and $\mathrm{Var}_{\Phi}(\mathrm{EC})$ can be written as

$$\begin{aligned} \mathrm{Var}_{\Phi}(\mathrm{IC}) &= \sum_{m=1}^{3} \mathrm{Var}_{\Phi_{mm}}(\mathrm{IC}_{mm}) \text{ and} \\ \mathrm{Var}_{\Phi}(\mathrm{EC}) &= \sum_{m=1}^{3} \mathrm{Var}_{\Phi_{mm}}(\mathrm{EC}_{mm}). \end{aligned} \tag{11}$$

Eq. (11) indicates that the variations of IC and EC are equal to summation of variations of their respective IC_{mm} and EC_{mm}, where IC_{mm} and EC_{mm} are from one luminance ($m = 1$) and others ($m = 2,3$) are from two chrominances. This confers important implication about color effect on variation ratio: two chrominances can make independent contribution to construct intra- and extra-personal variations, denoted as $\mathrm{Var}_{\Phi}(\mathrm{IC})$ and $\mathrm{Var}_{\Phi}(\mathrm{EC})$, of feature subspace in the separate manner with luminance. On the contrary, in the traditional gray-scale based eigenface FR, distribution of intra- and extra-personal variations ($\mathrm{Var}_{\Phi_{11}}(\mathrm{IC}_{11})$ and $\mathrm{Var}_{\Phi_{11}}(\mathrm{EC}_{11})$) in the feature subspace spanned by Φ_{11} are totally determined by statistical characteristic of only luminance.

4. Effect of color and face resolution

In this section, we exploit how color affects on variation ratio with respect to changes in face resolution. From Eq. (11), $\mathrm{Var}_{\Phi}(\mathrm{IC})$ and $\mathrm{Var}_{\Phi}(\mathrm{EC})$ consists of three independent intra- and extra-personal variations, denoted as $\mathrm{Var}_{\Phi_{mm}}(\mathrm{IC}_{mm})$ and $\mathrm{Var}_{\Phi_{mm}}(\mathrm{EC}_{mm})$, where $m = 1,2,3$. Since each spectral component of skin-tone color have different inherent property [21], it is reasonable to assume that respective $\mathrm{Var}_{\Phi_{mm}}(\mathrm{IC}_{mm})$ and $\mathrm{Var}_{\Phi_{mm}}(\mathrm{EC}_{mm})$ is differently changed over face resolution variation. Especially, it was well-known that the chromatic contrast sensitivity is mostly concentrated on low-spatial frequency regions compared to luminance [9], [22]. It means intrinsic features of color are robust to decrease of face resolution. Therefore, two chrominance components in Eq. (11) can play a supplement role in compensating degraded variation ratio caused by loss of discriminative features of luminance due to resolution reduction.

To measure the increase of variation ratio induced by chrominance information with respect to face resolution change, we propose the VRG. Using Eq. (4) and (11), the variation ratio, parameterized by face resolution (γ), for gray-scale based feature subspace is defined as

$$\mathrm{J}^{\mathrm{lum}}(\gamma) = \frac{\mathrm{Var}_{\Phi_{11}(\gamma)}(\mathrm{EC}_{11}(\gamma))}{\mathrm{Var}_{\Phi_{11}(\gamma)}(\mathrm{IC}_{11}(\gamma))}. \tag{12}$$

On the other hand, the variation ratio for color augmentation based feature subspace is defined as

$$\mathrm{J}^{\mathrm{lum+chrom}}(\gamma) = \frac{\mathrm{Var}_{\Phi(\gamma)}(\mathrm{EC}(\gamma))}{\mathrm{Var}_{\Phi(\gamma)}(\mathrm{IC}(\gamma))} = \frac{\sum_{m=1}^{3} \mathrm{Var}_{\Phi_{mm}(\gamma)}(\mathrm{EC}_{mm}(\gamma))}{\sum_{m=1}^{3} \mathrm{Var}_{\Phi_{mm}(\gamma)}(\mathrm{IC}_{mm}(\gamma))}. \tag{13}$$

Finally, VRG with respect to γ is defined as

$$\mathrm{VRG}(\gamma) = \frac{\mathrm{J}^{\mathrm{lum+chrom}}(\gamma) - \mathrm{J}^{\mathrm{lum}}(\gamma)}{\mathrm{J}^{\mathrm{lum}}(\gamma)} \times 100. \tag{14}$$

$\mathrm{VRG}(\gamma)$ represents the relative amounts of variation ratio increased by chrominances compared to one from luminance at face resolution γ. In other words, $\mathrm{VRG}(\gamma)$ can quantitatively measure the effect of color on performance improvement with varying face resolution γ.

To validate the effectiveness of VRG, we measure $\mathrm{J}^{\mathrm{lum}}(\gamma)$ and $\mathrm{J}^{\mathrm{lum+chrom}}(\gamma)$ in Eq. (14) with standard color face datasets (CMU PIE, FERET, and XM2VTSDB) by changing face resolution γ. The 5,000 images were first collected from three datasets. The 500 images were randomly selected from collected images and then used to compute variation ratios by using Eq. (12) and

(13). The selection process was repeated 20 times so that variation ratios computed here were the average of 20 random selections. For luminance and chrominance features, YC_bC_r color space was adopted since it is widely used in image and video compression standards.

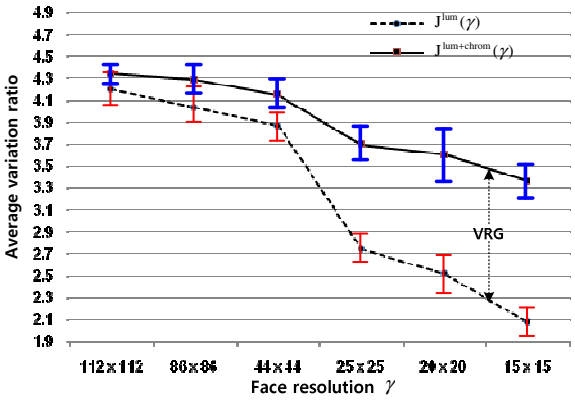

Figure 1. Average variation ratios and the corresponding standard deviations with respect to six different face resolution. Note that, margin between curves of $J^{lum}(\gamma)$ and $J^{lum+chrom}(\gamma)$ represents VRG defined as Eq. (14).

The results are shown in Figure 1. In Figure 1, $J^{lum}(\gamma)$ denotes average variation ratio calculated from luminance facial images with resolution γ, i.e., Y plane from YC_bC_r color space. In addition, $J^{lum+chrom}(\gamma)$ denotes average variation ratio computed from YC_bC_r configuration samples. To show the stability of measured variation ratios, standard deviations for all cases of $J^{lum}(\gamma)$ and $J^{lum+chrom}(\gamma)$ are also represented in Figure 1. As can be seen in Figure 1, at high-resolution (above 44×44), the margin between $J^{lum}(\gamma)$ and $J^{lum+chrom}(\gamma)$ is small since luminance is even more dominant than chrominances in determining $J^{lum+chrom}(\gamma)$. However, we can see that $J^{lum}(\gamma)$ noticeably fall off at low-resolution faces (25×25 or less) compared to ones computed from high-resolution faces (above 44×44). This is attributed to the fact that the extra-personal variation relying on distinctive features (e.g., edge) of gray-scale facial images between different subjects is significantly decreased as the faces have much lower resolution. On the other hand, $J^{lum+chrom}(\gamma)$ are slowly decreasing in relative to $J^{lum}(\gamma)$ even as the face resolution becomes much lower. Especially, it should be noted that $J^{lum+chrom}(\gamma)$ show much higher value than $J^{lum}(\gamma)$ at face resolution 25×25 or less. This result is due to the fact that luminance contrast sensitivity drops off at low spatial frequencies much faster than chromatic contrast sensitivity [22], [23]. Above results verify that VRG can be a relevant parameter, as theoretical point, that can explain well why role of color would be significant when low-resolution faces are applied to subspace FR methods such as PCA.

5. Experiments

In this section, extensive experiments have been carried out to investigate the contribution of color to the performance improvement with various face resolutions. To form training and probe sets, total 3,192 facial images from 341 subjects were collected from three public datasets. For this, 1,428 frontal view images of 68 subjects was collected from CMU PIE; for one subject, images had 21 different lighting variations with 'room lighting on' conditions. From Color FERET, the 700 frontal view images of 140 subjects (5 samples/subject) were collected from **fa, fb, fc,** and **dup1** sets [17]. From XM2VTSDB, 1,064 frontal view images of 133 subjects were obtained from two different sessions [18]; each subject includes eight facial images which contain illumination and resolution variations. Also, we constructed gallery set composed of 341 different samples corresponding 341 different subjects to be identified. Note that gallery images have neutral illumination and expression [17]. To see the role of color in terms of face resolution, we carried out resizing over the collected DB sets to get various face resolutions. To cover face resolutions from practical still image- to video-based FR applications published in previous works [5-7], the six different face resolutions were used: 112×112, 86×86, 44×44, 25×25, 20×20, and 15×15 (pixels). Figure 2 shows examples of facial images containing face resolution variations.

Figure 2. The examples of facial images from Color FERET according to six different face resolutions.

For the gray-scale face images, R [13] channel from RGB color space was used. To form the spectral component configurations, chrominance components from YC_bC_r, YIQ, and L*a*b* color spaces were used

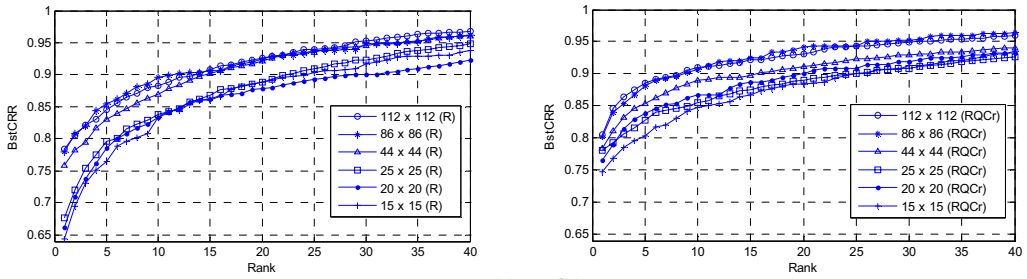

(a) PCA

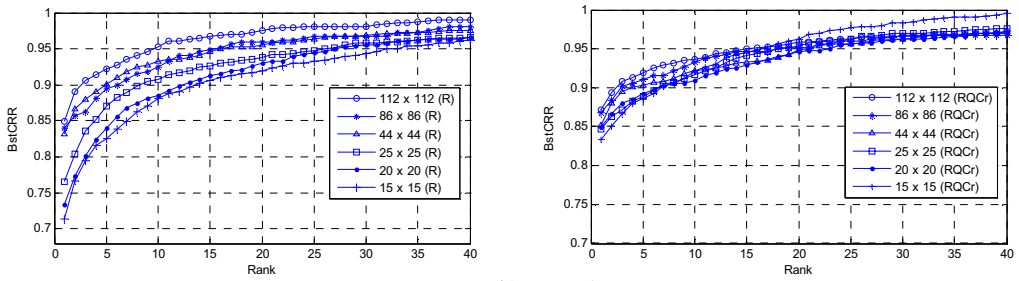

(b) FLDA

Figure 3. CMC curves with respect to six different face resolutions. The graphs in the left side are from gray-scale, while thoses in the right side are from the best spectral component configurations for each resolution.

for combination with gray-scale feature. Table 1 shows gray-scale and chrominances from four different color spaces and the kinds of spectral component configurations used for experiments.

Table 1. Color spaces and the types of spectral component configurations used for experiments.

Gray-scale	R from RGB [13]
Chrominances	C_bC_r [11] from YCbCr (4:4:4)
	IQ [11] from YIQ
	a*b* [12] from L*a*b*
	QC_r [11] from YIQ and YC_bC_r (4:4:4)
Spectral component configurations	RC_bC_r
	RIQ
	Ra*b*
	RQC_r

To show the stability of the experimental results about color effect on face resolutions regardless of FR algorithms, PCA and FLDA were utilized to perform the experiments. In subspace FR methods such as PCA and FLDA, the recognition performance relies heavily on the number of linear subspace dimension (feature dimension) [20]. So, the subspace dimension should be carefully chosen and then fixed over six different face resolutions to make fair comparison of performance. For PCA and PCA process in FLDA, a well-known 95% energy capturing rule [20] is adopted to determine subspace dimension. In these experiments, the number of training samples was 1,023 images so that subspace dimension was experimentally determined as 200 to satisfy 95% energy capturing rule.

For similarity metrics in PCA and FLDA, Mahalanobis and Euclidean distance were used, respectively. In FR tasks, performance results should be reported for identification and verification. Identification performance is usually plotted on Cumulative Match Characteristic (CMC) curve [17]. The horizontal axis of the CMC curves is rank, while vertical axis is the identification rate. The Best Found Correct Recognition Rate (BstCRR) [20] was adopted as identification rate for fair comparison. For verification performance, Face Verification Rate (FVR) versus the False Accept Rate (FAR) was used. For an experimental protocol, collected set of 3,192 facial images was randomly partitioned into two sets: training and probe sets. The training set consisted of (3 *samples* × 341 *subjects*) images, while probe set consisted of the rest of images which have at least 2 samples per one subject. There was no overlapping between two sets. To guarantee reliability of the evaluation, 20 runs of random partitions were executed, and all of the experimental results reported here were averaged over 20 runs.

Figure 3 shows CMC curves with respect to six different face resolutions as well as corresponding the best spectral component configurations in PCA and FLDA. It should be noted that face resolution of each pair of training, gallery, and probe sets were all the same in Figure 3. From Figure 3, RQC_r shows the best performance of all spectral component configurations described in Table 1 in all face resolutions and used FR

algorithms. This result is consistent with previous work [11] that reported QC_r is the best chrominances in FRGC (Face Recognition Grand Challenge) [11] database and evaluation frameworks. From Figure 3, we can observe that there is a little difference in the BstCRR performance with 112×112, 86×86, and 44×44 gray-scale facial images, while BstCRR performance is tended to be deteriorated with 25×25 and below gray-scale ones in both FR algorithms. In specific, BstCRR difference between 112×112 and 15×15 gray-scale facial images are 14.05% and 13.60% at rank 1 in PCA and FLDA, respectively. In case of color features shown in the right side in Figure 3, we can see that color information contributes to the BstCRR improvement compared to gray-scale in all face resolutions. Especially, effect of color becomes significant as the face resolution are 25×25 and below. Compared to gray-scale cases, performance margins between 112×112 and 15×15 are reduced to 5.71% and 3.78% at rank 1 in PCA and FLDA, respectively.

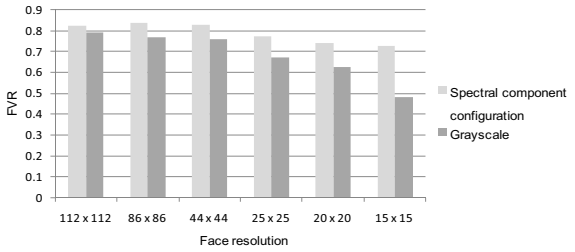

(a) PCA

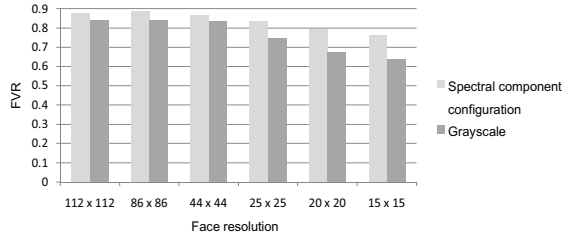

(b) FLDA

Figure 4. Comparisons of FVR at FAR 0.1% with respect to six different face resolutions.

Figure 4 shows FVRs at FAR 0.1% with varying face resolutions. Like the results in Table 2, RQC_r achieved the best FVRs in all face resolutions from Figure 4. As can be seen in Figure 4, color information can have a great impact on FVR improvement at low-resolution facial images (below 25×25) compared to high-resolution ones. For example, when 112×112 high-resolution images are applied to PCA and FLDA, 3.55% and 5.67% FVR improvement at FAR 0.1% are obtained from color information, respectively, while, in case of 15×15 low-resolution ones, color cues increase 24.43% and 16.27% at FAR 0.1% in relative to corresponding FVRs from gray-scale, respectively.

Table 2. Comparison of VRGs with respect to six different face resolutions in PCA. Note that unit of VRG(γ) is %.

Face resolution γ	112x112	86x86	44x44	25x25	20x20	15x15
VRG(γ)	3.80	4.20	9.80	55.20	69.90	71.20

Table 2 shows the comparison of VRGs in Eq. (14) with respect to six different face resolutions. In Table 3, gray-scale and spectral component configurations used for each resolution are the same as ones in Figure 3. From Table 2, VRG(γ) are relatively small in cases of high-resolution, i.e., 44×44 or higher. This result is attributed to dominance of gray-scale information at high-resolution to build extra-personal variation in the feature subspace. So, the contribution of color is comparatively small. On the other hand, in case of low-resolution, i.e., 25×25 or below, VRG(γ) become large. This result indicates that color information can compensate decreased extra-personal variation induced by resolution reduction in the feature subspace.

6. Conclusion

In this paper, we exploit the effect of color on FR performance with varying face resolution. We found the role of color becomes significant as the face resolution is getting lower. Another interesting finding is that the recognition performance resulting from low-resolution color faces is comparable to those coming from high-resolution gray-scale faces. Theoretical analysis and experimental results verified that the proposed color-based FR framework is very useful in FR applications with which low-resolution faces are commonly encountered, especially promising face annotation applications on video-clips and personal photos via Web services.

Appendix

Let $I\Phi_{mm}$ and $I\Lambda_{mm}$ be eigenvector and corresponding diagonal eigenvalue matrices of IC_{mm} in Eq. (7), where $m=1,2,3$. That is

$$\mathrm{I}\Phi_{mm}^{\mathrm{T}}\mathrm{IC}_{mm}\mathrm{I}\Phi_{mm}=\mathrm{I}\Lambda_{mm}. \quad (A.1)$$

Using $\mathrm{I}\Phi_{mm}$ $(m=1,2,3)$, we define a block diagonal matrix Q as

$$\mathrm{Q}=\mathrm{diag}(\mathrm{I}\Phi_{11},\mathrm{I}\Phi_{22},\mathrm{I}\Phi_{33}). \quad (A.2)$$

Note that Q is an orthogonal matrix. Using Eq. (6) and (A.2), matrix IS is defined as

$$\mathrm{IS}=\mathrm{Q}^{\mathrm{T}}\,\mathrm{IC}\,\mathrm{Q}$$
$$=\begin{bmatrix}\mathrm{I}\Lambda_{11} & \mathrm{I}\Phi_{11}^{\mathrm{T}}\mathrm{IC}_{12}\mathrm{I}\Phi_{22} & \mathrm{I}\Phi_{11}^{\mathrm{T}}\mathrm{IC}_{13}\mathrm{I}\Phi_{33}\\ \mathrm{I}\Phi_{22}^{\mathrm{T}}\mathrm{IC}_{21}\mathrm{I}\Phi_{11} & \mathrm{I}\Lambda_{22} & \mathrm{I}\Phi_{22}^{\mathrm{T}}\mathrm{IC}_{23}\mathrm{I}\Phi_{33}\\ \mathrm{I}\Phi_{33}^{\mathrm{T}}\mathrm{IC}_{31}\mathrm{I}\Phi_{11} & \mathrm{I}\Phi_{33}^{\mathrm{T}}\mathrm{IC}_{32}\mathrm{I}\Phi_{22} & \mathrm{I}\Lambda_{33}\end{bmatrix}. \quad (A.3)$$

IS in Eq. (A.3) is similar to IC since there exists an invertible matrix Q satisfying $\mathrm{IS}=\mathrm{Q}^{-1}\,\mathrm{ICQ}=\mathrm{Q}^{\mathrm{T}}\,\mathrm{ICQ},$ where $\mathrm{Q}^{-1}=\mathrm{Q}^{\mathrm{T}}$. Due to *similarity*, IS and IC have the same eigenvalues and trace value such that $\mathrm{tr}(\mathrm{IS})=\mathrm{tr}(\mathrm{IC})$. Note that $\mathrm{tr}(\mathrm{I}\Lambda_{mm})$ is the sum of eigenvalues of IC_{mm}. Using $\mathrm{tr}(\mathrm{IS})=\mathrm{tr}(\mathrm{IC}),$ $\mathrm{tr}(\mathrm{IC})$ can be written as

$$\mathrm{tr}(\mathrm{IC})=\sum_{m=1}^{3}\mathrm{tr}(\mathrm{I}\Lambda_{mm}). \quad (A.4)$$

Similar analysis of Eq. (A.1), (A.2), and (A.3) is also easily applied to EC shown in Eq. (5). That is, $\mathrm{tr}(\mathrm{EC})$ can written as

$$\mathrm{tr}(\mathrm{EC})=\sum_{m=1}^{3}\mathrm{tr}(\mathrm{E}\Lambda_{mm}), \quad (A.5)$$

where $\mathrm{E}\Lambda_{mm}$ ($m=1,2,3$) is a diagonal eigenvalue matrix of EC_{mm}.

7. Reference

[1] Z. Zhu, S. C.H. Hoi, and M. R. Lyu, "Face Annotation Using Transductive Kernel Fisher Discriminant", *IEEE Trans. Multimedia*, vol. 10, no. 1, pp. 86-96, 2008.

[2] W. Zhao, R. Chellappa, P. J. Phillips, and A. Rosenfeld, "Face Recognition: A Literature Survey", *ACM Comput. Surv.,* vol. 35, no. 4, pp. 399-458, 2003.

[3] D. M. Blackburn, J. M. Bone, and P. J. Phillips, "Face Recognition Vendor Test 2000 Evaluation Report", 2001.

[4] J.H. Lim and J.S. Jin, "Semantic indexing and retrieval of home photos", *Proc. of IEEE Int'l conf. on ICARCV*, 2007.

[5] H. K. Ekenel, A. Pnevmatikakis, "Video-Based Face Recognition Evaluation in the CHIL Project – Run1", *Proc. IEEE Int'l Conf. Automatic Face and Gesture Recognition,* 2006.

[6] B. J. Boom, G. M. Beumer, L. J. Spreeuwers, and R. N. J. Veldhuis, "The Effect of Image Resolution on the Performance of a Face Recongition System", *Proc. IEEE. Int'l Conf. Control, Automation, Robotics, and Vision*, 2006.

[7] A. Hadid and M. Pietikainen, "From Still Image to Video-Based Face Recognition: An Experimental Analysis", *Proc. Int'l. Conf Automatic Face and Gesture Recognition*, 2004.

[8] L. H. Wurm, G. E. Legge, L. M. Isenberg, and A. Lubeker, "Color improves object recognition in normal and low vision", *Journal of Experimental Psychology: Human Perception and Performance*, vol. 19, pp. 899-911,1993.

[9] A. Yip and P. Sinha, "Role of color in face recognition", *Journal of Vision*, vol. 2, no. 7, pp. 596-596a, 2002.

[10] L. Torres, J. Y. Reutter, and L. Lorente, "The importance of the color information in face recognition", *Proc. IEEE Int'l Conf. Image Processing*, 1999.

[11] P. Shih and C. Liu, "Improving the Face Recognition Grand Challenge Baseline Performance using Color Configurations Across Color Spaces", *Proc. IEEE Int'l Conf. Image Processing*, 2006.

[12] P. Shih and C. Liu, "Comparative assessment of content-based face image retrieval in different color spaces", *International Journal of Pattern Recognition and Artificial Intelligence*, vol. 19, no. 7, pp. 873-893, 2005.

[13] M. T. Sadeghi, S. Khoushrou, and J. Kittler, "Confidence based gating of colour features for face authentication", *Proc. Int'l Workshop Multiple Classifier System*, 2007.

[14] M. A. Turk and A. P. Pentland, "Eigenfaces for Recognition", *J. Cognitive Neurosci*., vol. 3, no. 1, pp. 71-86, 1991.

[15] P. N. Belhumeur, J. P. Hesphanha, and D. J. Kriegman, "Eigenfaces vs. Fisherfaces: Recognition Using Class Specific Linear Projection", *IEEE Trans. Pattern. Anal. Machine Intell.*, vo1. 9, no. 7, pp. 711-720, 1997.

[16] T. Sim, S. Baker, and M. Bsat, "The CMU Pose, Illumination, and Expression Database", *IEEE Trans. Pattern Anal. Mach. Intell*., vol. 25, no. 12, pp. 1615-1618, 2003.

[17] P. J. Phillips, H. Moon, S. A. Rizvi, and P. J. Rauss, "The FERET Evaluation Methodology for Face Recognition Algorithms", *IEEE Trans. Pattern Anal. Mach. Intell*., vol. 22, no. 10, pp. 1090-1104, 2000.

[18] K. Messer, J. Mastas, J. Kittler, J. Luettin, and G. Maitre, "XM2VTSDB: The Extended M2VTS Database", *Proc. Int'l Conf. Audio- and Video-Based Biometric Person Authentication*, 1999.

[19] X. Wang and X. Tang, "A Unified Framework for Subspace Face Recognition", *IEEE Trans. Pattern Anal. Mach. Intell.*, vol. 26, no. 9, pp. 1222-1228, 2004.

[20] J. Wang, K. N. Plataniotis, and A. N. Venetasanopoulos, "Selecting discriminant eigenfaces for face recognition", *Pattern Recognit., Lett.,* vol. 26, no. 10, pp. 1470-1482, 2005.

[21] R. Hsu. M. A. Monttaleb, and A. Jain, "Face Detection in Color Images," *IEEE Trans. Pattern Anal. Mach. Intell*., vol. 24, no. 5, pp. 696-706, 2002.

[22] D. H. Kelly, "Spatiotemporal variation of chromatic and achromatic contrast thresholds", *Journal of Optical Society of America*, vol. 73, pp. 742-749, 1983.

[23] J. B. Derrico and G. Buchsbaum, "A computational model of spatiochromatic image coding in early vision", *Journal of Visual Communication and Image Representation*, vol. 2, pp. 31-38, 1991.